Research Paper

Association between bone mineral density and brain parenchymal atrophy and ventricular enlargement in healthy individuals

In-Suk Bae[1], Jae Min Kim[1], Jin Hwan Cheong[1], Je Il Ryu[1], Myung-Hoon Han[1]

[1]Department of Neurosurgery, Hanyang University Guri Hospital, Guri, Gyonggi-do, Korea

Correspondence to: Myung-Hoon Han; **email:** gksmh80@gmail.com
Keywords: cerebral atrophy, ventricular enlargement, osteoporosis, bone mineral density
Received: April 7, 2019 **Accepted:** September 21, 2019 **Published:** September 30, 2019

ABSTRACT

Bone, vascular smooth muscle, and arachnoid trabeculae are composed of the same type of collagen. However, no studies have investigated the relationship between bone mineral density deterioration and cerebral atrophy, both of which occur in normal, healthy aging. Accordingly, we evaluated whether bone mineral density was associated with brain parenchymal atrophy and ventricular enlargement in healthy individuals. Intracranial cavity, brain parenchyma, and lateral ventricles volumes were measured using brain magnetic resonance imaging (MRI) with a semiautomated tool. We included 267 individuals with no history of dementia or other neurological diseases, who underwent one or more dual-energy X-ray absorptiometry scans and brain MRIs simultaneously (within 3 years of each other) at our hospital over an 11-year period. We found that progression of brain parenchymal atrophy was positively associated with bone mineral density after full adjustment (B, 0.94; P < 0.001). In addition, individuals with osteoporosis showed more parenchymal atrophy among those younger than 80 years. In addition, we observed greater ventricular enlargement in individuals with osteoporosis among those older than 80 years. We believe that osteoporosis may play a role in the acceleration of parenchymal atrophy during the early-stages, and ventricular enlargement in the late-stages, of normal aging-related cerebral atrophy.

INTRODUCTION

Cerebral atrophy and ventricular enlargement which occur during the normal aging process are known to lead to dementia, memory disorders, and cognitive impairment [1]. Physiological aging of the brain is at an increased risk of dementia, and addressing this public health problem is a major challenge currently facing medical research [2].

Bone, blood vessels, and arachnoid trabeculae share the same collagen type (type 1 collagen) [3–5]. Osteogenesis imperfecta, a disease caused by mutations in genes encoding type 1 collagen, affects the cardio- or cerebrovascular and ventricular systems, as well as bone [6–9]. Osteoporosis is a systemic disease that is strongly associated with genes that encode for the components of type 1 collagen [10, 11].

To the best of our knowledge, there are no studies investigating the association between bone mineral density (BMD) and cerebral atrophy in healthy individuals. As bone, vascular smooth muscle, and arachnoid trabeculae are composed of the same type of collagen, we hypothesized that osteoporosis may be linked to brain parenchymal atrophy and ventricular enlargement in the process of normal aging-related cerebral atrophy. Therefore, we investigated this notion by analyzing T-scores from dual-energy X-ray absorptiometry (DXA) and measuring the intracranial cavity volume (ICV), brain parenchymal volume (BPV), and lateral ventricles volume (LVV) from brain magnetic

resonance imaging (MRI) using a 3D slicer software in healthy individuals.

RESULTS

Characteristics of study individuals

The average age of the subjects was 67.4 years, and 81.3% of individuals were women. A total of 72 individuals had osteoporosis and the overall mean T-score was −1.6. The mean ICV, BPV, and LVV were 1224.9 cc, 1026.4 cc, and 29.3 cc, respectively. The mean volume percentages of the brain parenchyma and lateral ventricles to the intracranial cavity were 83.8% and 2.4%, respectively. We found significant differences in ICV, BPV, LVV, and the intracranial cavity volume percentages of the brain parenchyma ((BPV/ICV) × 100(%)) and lateral ventricles ((LVV/ICV) × 100(%)) between subjects with osteoporosis and those without. Further descriptive data are shown in Table 1.

Detailed information on the bone densitometric parameters including bone mineral content (BMC), BMD, T-, and Z-score in the study participants classified by age group are also presented in Table 2. In addition, we assessed the relationships between volume percentage of brain parenchyma and lateral ventricles and different bone densitometric parameters using Pearson correlation analysis with/without adjustment for age (Tables 3 and 4).

Association between T-score and volume percentages of the brain parenchyma and lateral ventricles to the intracranial cavity

Figure 1 shows significant positive and negative correlations between T-scores and the intracranial cavity volume percentages of the brain parenchyma and lateral ventricles. We observed a statistically significant increase in the intracranial cavity volume percentage of the brain parenchyma ((BPV/ICV)×100(%)) with increasing T-scores (B, 1.400; P<0.001) (Figure 1A). Conversely, T-scores were negatively associated with intracranial cavity volume percentages of the lateral ventricles ((LVV/ICV)×100(%)) (B, −0.222; P<0.001) (Figure 1B). After adjusting for all covariates including age, we observed an independent positive correlation between T-scores and intracranial cavity volume percentages of the brain parenchyma, with an approximate increase of 0.9 % per 1 T-score increase (B, 0.94; 95% CI, 0.48 to 1.40; P<0.001; Table 5). However, percentage of lateral ventricles showed no significant association with T-score in the multivariable linear analysis (B, −0.06; 95% CI, −0.18 to 0.06; P=0.339).

Other factors associated with volume percentages of the brain parenchyma and lateral ventricles

As expected, age was independently associated with volume percentages of the brain parenchyma and lateral ventricles (B, −0.15; 95% CI, −0.20 to −0.10; P<0.001; B, 0.04; 95% CI, 0.03 to 0.05; P<0.001, respectively; Table 5). Diabetes was an independent predictor of lower volume percentages of the brain parenchyma (B, −1.41; 95% CI, −2.47 to −0.35; P=0.009). In addition, we observed a statistically significant decrease in the volume percentage of lateral ventricles with an increasing body mass index (BMI) (B, −0.05; 95% CI, −0.09 to −0.02; P=0.007). We additionally investigated the association between T-score and BMI in the study participants (Supplementary Figure 1).

Comparison of volume percentage of brain parenchyma and lateral ventricles between age groups according to osteoporosis

The boxplot shows a statistically significant tendency of lower intracranial cavity volume percentage of the brain parenchyma in individuals with osteoporosis among those under 80 years of age (Figure 2A). However, there was no difference of volume percentage of brain parenchyma between individuals with and without osteoporosis in individuals older than 80 years. Surprisingly, we found a significant higher volume percentage of lateral ventricles in individuals with osteoporosis among those older than 80 years (Figure 2B). However, there were no significant differences of volume percentage of lateral ventricles between individuals with and without osteoporosis among those under 80 years. We also observed similar tendencies in associations when the study participants were categorized into normal, osteopenia, and osteoporosis groups (Figure 2C and 2D). We further evaluated those relationships based on sex and age groups. Similar tendencies in associations were observed in the female group (Figure 3A and 3B). However, male participants showed no significant differences in volume percentage of brain parenchyma and lateral ventricles between individuals with and without osteoporosis, which is thought to be due to a low sample size (Figure 3C and 3D). When study participants were divided into different age groups, we observed an overall tendency towards a lower volume percentage of brain parenchyma in individuals with osteoporosis among those under 80 years of age and higher volume percentage of lateral ventricles in individuals with osteoporosis among those older than 80 years (Figure 4).

Table 6 shows the characteristics of the study participants classified by age group. We observed a significant decrease in T-score with a higher age group. The mean

Table 1. Characteristics of the study individuals according to osteoporosis.

Characteristics	Osteoporosis (-)	Osteoporosis (+)	Total	P
Number	195	72	267	
Sex, female, n (%)	159 (81.5)	58 (80.6)	217 (81.3)	0.995
Age at the time of brain MRI, mean ± SD, y	65.4 ± 12.3	72.7 ± 9.3	67.4 ± 12.0	<0.001
Time interval between brain MRI and DXA, median (IQR), days	193.0 (35.0–486.0)	154.5 (22.0–363.5)	184.0 (33.0–441.0)	0.077
ICV, mean ± SD, cc	1232.7 ± 90.7	1203.9 ± 89.9	1224.9 ± 91.2	0.021
BPV, mean ± SD, cc	1042.1 ± 98.8	983.8 ± 79.5	1026.4 ± 97.3	< 0.001
LVV, mean ± SD, cc	27.9 ± 14.2	33.1 ± 16.4	29.3 ± 15.0	0.011
Volume percentage of the brain parenchyma ((BPV/ICV)×100), mean ± SD, %	84.5 ± 4.7	81.8 ± 3.9	83.8 ± 4.6	< 0.001
Volume percentage of the lateral ventricles ((LVV/ICV)×100), mean ± SD, %	2.3 ± 1.1	2.8 ± 1.4	2.4 ± 1.2	0.007
T-score, mean ± SD	-1.1 ± 0.9	-3.0 ± 0.5	-1.6 ± 1.2	< 0.001
Lumbar spine	-0.7 ± 1.2	-2.8 ± 0.7	-1.3 ± 1.5	< 0.001
Femur neck	-0.6 ± 1.2	-2.1 ± 1.0	-1.0 ± 1.3	< 0.001
BMI, mean ± SD, kg/m^2	24.5 ± 3.5	22.5 ± 3.5	24.0 ± 3.6	< 0.001
Height, mean ± SD, cm	156.4 ± 8.0	152.8 ± 7.9	155.4 ± 8.1	0.001
Weight, mean ± SD, kg	59.9 ± 9.6	52.5 ± 8.3	57.9 ± 9.8	< 0.001
Hypertension, n (%)	91 (46.7)	39 (54.2)	130 (48.7)	0.342
Diabetes, n (%)	68 (34.9)	19 (26.4)	87 (32.6)	0.244
Alcohol, n (%)	27 (13.8)	7 (9.7)	34 (12.7)	0.490
Smoking, n (%)	14 (7.2)	9 (12.5)	23 (8.6)	0.259

SD: standard deviation; MRI: magnetic resonance imaging; DXA: dual-energy X-ray absorptiometry; IQR: interquartile range; ICV: intracranial cavity volume; BPV: brain parenchymal volume; LVV: lateral ventricles volume; BMI: body mass index.

Table 2. Descriptive statistics of bone densitometric parameters in the study participants classified by age group.

Bone densitometric parameters	< 65 y (n=95)	65 y–79 y (n=131)	80 y or older (n=41)	Total (n=267)	P
Femur neck T-score, mean ± SD	-0.35 ± 1.24	-1.16 ± 1.15	-1.96 ± 1.18	-1.00 ± 1.31	< 0.001
Lumbar spine T-score, mean ± SD	-0.94 ± 1.42	-1.41 ± 1.48	-1.79 ± 1.25	-1.30 ± 1.45	0.003
T-score (lower value between the lumbar spine and femoral neck), mean ± SD	-1.14 ± 1.24	-1.76 ± 1.10	-2.31 ± 1.01	-1.63 ± 1.21	< 0.001
Femur neck BMC, mean ± SD, g	28.76 ± 6.66	26.74 ± 7.80	23.82 ± 8.32	27.01 ± 7.65	0.002
Lumbar spine BMC, mean ± SD, g	54.63 ± 14.22	48.71 ± 17.70	45.33 ± 15.88	50.30 ± 16.56	0.003
Femur neck BMD, mean ± SD, g/cm^2	0.83 ± 0.14	0.74 ± 0.13	0.64 ± 0.15	0.75 ± 0.15	< 0.001
Lumbar spine BMD, mean ± SD, g/cm^2	0.90 ± 0.16	0.85 ± 0.18	0.80 ± 0.15	0.86 ± 0.17	0.004
Femur neck Z-score, mean ± SD	0.26 ± 1.22	0.20 ± 0.96	-0.11 ± 1.12	0.17 ± 1.09	0.191
Lumbar spine Z-score, mean ± SD	0.13 ± 1.16	0.54 ± 1.07	0.51 ± 0.93	0.39 ± 1.10	0.014

SD: standard deviation; BMC: bone mineral content; BMD: bone mineral density.

Table 3. Pearson correlation coefficients among the volume percentage of brain parenchyma and lateral ventricles to the intracranial cavity and bone densitometric parameters of the study cohort.

	Volume percentage of the brain parenchyma ((BPV/ICV) × 100%)	Volume percentage of the lateral ventricles ((LVV/ICV) × 100%)	Femur neck T-score	Lumbar spine T-score	T-score (lower value between the lumbar spine and femoral neck)	Femur neck BMC	Lumbar spine BMC	Femur neck BMD	Lumbar spine BMD	Femur neck Z-score	Lumbar spine Z-score
Volume percentage of the brain parenchyma ((BPV/ICV) × 100%)	1	-0.418**	0.261**	0.321**	0.365**	0.131*	0.193**	0.262**	0.310**	0.115	0.122*
Volume percentage of the lateral ventricles ((LVV/ICV) × 100%)		1	-0.254**	-0.151*	-0.219**	-0.080	-0.062	-0.242**	-0.144*	-0.115	-0.017
Femur neck T-score			1	0.594**	0.782**	0.615**	0.499**	0.906**	0.593**	0.816**	0.408**
Lumbar spine T-score				1	0.888**	0.481**	0.764**	0.621**	0.987**	0.538**	0.829**
T-score (lower value between the lumbar spine and femoral neck)					1	0.574**	0.703**	0.808**	0.882**	0.710**	0.692**
Femur neck BMC						1	0.624**	0.767**	0.504**	0.563**	0.218**
Lumbar spine BMC							1	0.592**	0.780**	0.382**	0.484**
Femur neck BMD								1	0.632**	0.843**	0.382**
Lumbar spine BMD									1	0.537**	0.825**
Femur neck Z-score										1	0.589**
Lumbar spine Z-score											1

ICV: intracranial cavity volume; BPV: brain parenchymal volume; LVV: lateral ventricles volume; BMC: bone mineral content; BMD: bone mineral density *P<0.05 **P<0.01

Table 4. Age-adjusted Pearson correlation coefficients among the volume percentage of brain parenchyma and lateral ventricles to the intracranial cavity and bone densitometric parameters of the study cohort.

	Volume percentage of the brain parenchyma ((BPV/ICV) × 100%)	Volume percentage of the lateral ventricles ((LVV/ICV) × 100%)	Femur neck T-score	Lumbar spine T-score	T-score (lower value between the lumbar spine and femoral neck)	Femur neck BMC	Lumbar spine BMC	Femur neck BMD	Lumbar spine BMD	Femur neck Z-score	Lumbar spine Z-score
Volume percentage of the brain parenchyma ((BPV/ICV) × 100%)	1	-0.251**	0.075	0.249**	0.233**	0.048	0.104	0.081	0.239**	0.099	0.245**
Volume percentage of the lateral ventricles ((LVV/ICV) × 100%)		1	-0.066	-0.051	-0.054	0.012	0.048	-0.056	-0.045	-0.099	-0.123*
Femur neck T-score			1	0.564**	0.743**	0.602**	0.459**	0.886**	0.565**	0.877**	0.551**
Lumbar spine T-score				1	0.888**	0.458**	0.752**	0.594**	0.986**	0.540**	0.912**
T-score (lower value between the lumbar spine and femoral neck)					1	0.552**	0.686**	0.774**	0.883**	0.741**	0.834**
Femur neck BMC						1	0.608**	0.770**	0.482**	0.563**	0.264**
Lumbar spine BMC							1	0.564**	0.769**	0.379**	0.549**
Femur neck BMD								1	0.608**	0.902**	0.517**
Lumbar spine BMD									1	0.538**	0.905**
Femur neck Z-score										1	0.612**
Lumbar spine Z-score											1

ICV: intracranial cavity volume; BPV: brain parenchymal volume; LVV: lateral ventricles volume; BMC: bone mineral content. BMD: bone mineral density *P<0.05 **P<0.01.

volume percentages of the brain parenchyma in age < 65 years, 65–79 years, and 80 years or older were 86.4%, 82.7%, and 81.1%, respectively. In addition, the mean volume percentage of the lateral ventricles according to the same age groups were 1.8%, 2.5%, and 3.4%, respectively. There were no significant differences in other clinical factors between age groups, except for hypertension.

Comparison of volume percentage of brain parenchyma and lateral ventricles according to medical history

Study participants were classified according to their medical conditions (smoking history was not included in the analysis due to low sample size) (Supplementary Figures 2–4). We found an overall tendency towards lower volume percentage of brain parenchyma and higher volume percentage of lateral ventricles in individuals with hypertension and diabetes. However, more significant differences in volume percentage of brain parenchyma and lateral ventricles were observed between individuals with and without osteoporosis in participants without hypertension and diabetes.

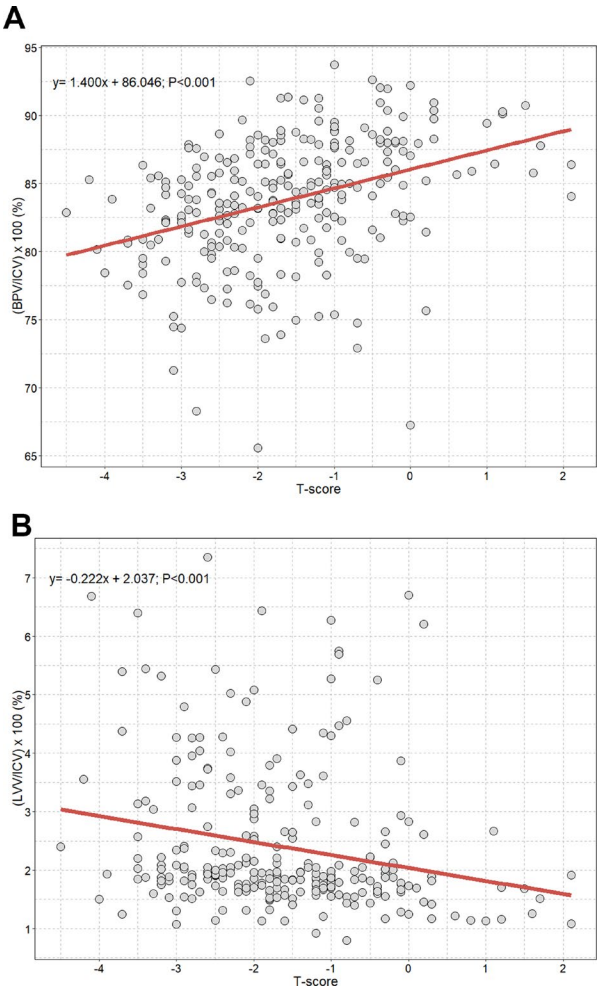

Figure 1. Scatterplot with linear regression line showing the association between T-score and volume percentages of brain parenchyma and lateral ventricles. (**A**) Volume percentage of brain parenchyma to intracranial cavity; (**B**) volume percentage of lateral ventricles to intracranial cavity. ICV=intracranial cavity volume: BPV=brain parenchymal volume; LVV=lateral ventricles volume.

DISCUSSION

We found that the progression of brain parenchymal atrophy was positively associated with bone mineral density after adjusting for covariates, including age, in healthy individuals. In addition, individuals with osteoporosis showed significantly lower intracranial cavity volume percentages of brain parenchyma among those under 80 years of age. On the contrary, we observed a significantly higher volume percentage of lateral ventricles in individuals with osteoporosis older than 80 years. To our knowledge, this study is the first to suggest that bone mineral density is related to brain parenchymal atrophy and ventricular enlargement in healthy individuals.

It is well known that brain atrophy and ventricular dilatation accelerate with increasing age [12]. The prevalence of dementias such as Alzheimer's disease increases exponentially after the age of 65 years [13]. A previous study of autopsy cases found that brain atrophy was detected in both normal individuals and patients with Alzheimer's-type dementia over 70 years of age [14]. However, the investigators observed that brain atrophy was accompanied by ventricular dilatation in all Alzheimer's-type dementia patients, but not in healthy individuals. Therefore, the authors concluded that brain atrophy may persist with increasing age whereas ventricular dilatation likely does not progress in healthy individuals; conversely, rapidly progressive brain atrophy with ventricular dilatation is likely a common characteristic of Alzheimer's-type dementia in patients over 70 years of age. A previous study revealed that patients with Alzheimer's disease had greater ventricular enlargement than subjects with mild cognitive impairment and normal elderly controls [15]. The authors suggested that ventricular enlargement represents a feasible short-term marker of disease progression in subjects with mild cognitive impairment and in those with Alzheimer's disease. Both normal aging and Alzheimer's disease are associated with changes in grey and white matter volume and white matter integrity, and it is hypothesized that Alzheimer's disease might simply reflect an accelerated aging process [16]; this makes, the separation between normal aging and Alzheimer's disease is frequently challenging.

Table 5. Multivariable linear regression analysis of the volume percentage of brain parenchyma and lateral ventricles to the intracranial cavity according to several clinical factors of the study cohort.

	Multivariable linear regression analysis			
	Volume percentage of the brain parenchyma ((BPV/ICV)×100%)		Volume percentage of the lateral ventricles ((LVV/ICV)×100%)	
Variable	β (95% CI)	P value	β (95% CI)	P value
Intercept	96.05		0.58	
Male (vs female)	-0.57 (-1.95 to 0.80)	0.412	0.40 (0.03 to 0.76)	0.033
Age at the time of brain MRI (per 1-year increase)	-0.15 (-0.20 to -0.10)	<0.001	0.04 (0.03 to 0.05)	<0.001
Time interval between brain MRI and DXA (per 1-month increase)	-0.01 (-0.06 to 0.04)	0.667	0.01 (-0.01 to 0.02)	0.291
T-score	0.94 (0.48 to 1.40)	<0.001	-0.06 (-0.18 to 0.06)	0.339
BMI (per 1 BMI increase)	-0.02 (-0.16 to 0.13)	0.840	-0.05 (-0.09 to -0.02)	0.007
Hypertension	0.53 (-0.59 to 1.65)	0.352	0.13 (-0.17 to 0.43)	0.397
Diabetes	-1.41 (-2.47 to -0.35)	0.009	0.17 (-0.11 to 0.45)	0.243
Alcohol	0.09 (-1.44 to 1.62)	0.910	0.16 (-0.24 to 0.57)	0.429
Smoking	0.33 (-1.53 to 2.19)	0.728	-0.43 (-0.93 to 0.07)	0.089

ICV: intracranial cavity volume; BPV: brain parenchymal volume; LVV: lateral ventricles volume; CI: confidence interval; MRI: magnetic resonance imaging; DXA: dual-energy X-ray absorptiometry; BMI: body mass index.

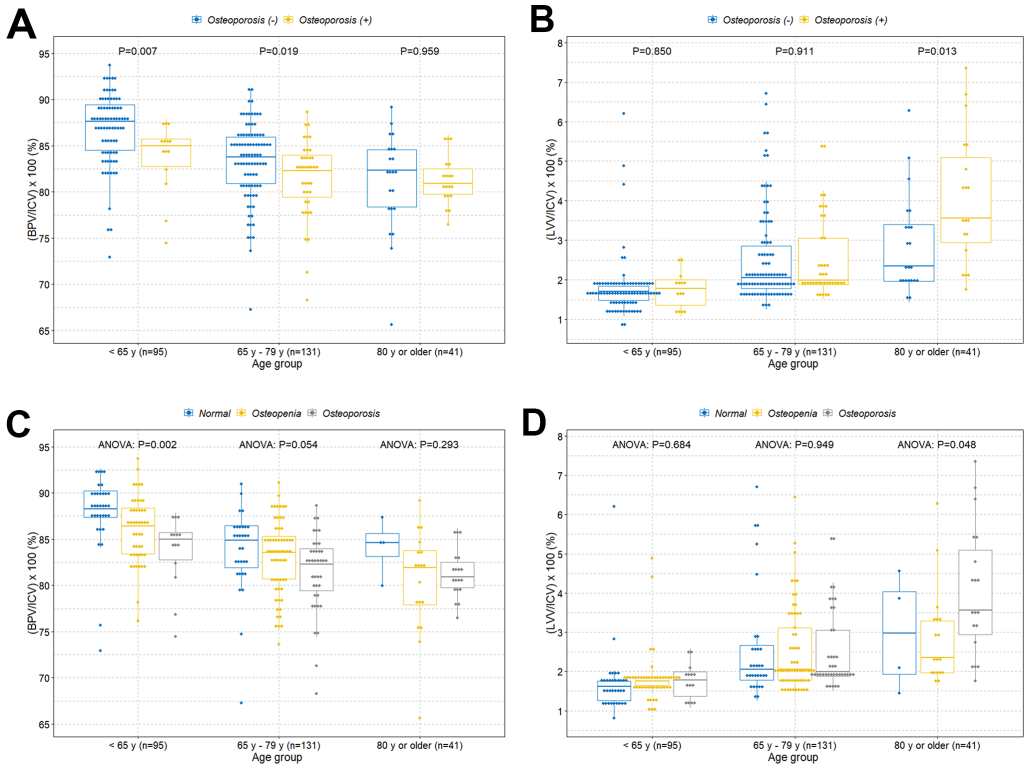

Figure 2. Boxplots with dot plots of the volume percentages of brain parenchyma and lateral ventricles classified by age groups according to two different BMD groups. (**A**) Volume percentage of brain parenchyma to intracranial cavity classified by age groups according to osteoporosis; (**B**) volume percentage of lateral ventricles to intracranial cavity classified by age groups according to osteoporosis; (**C**) volume percentage of brain parenchyma to intracranial cavity classified by age groups based on normal, osteopenia, and osteoporosis groups; (**D**) volume percentage of lateral ventricles to intracranial cavity classified by age groups based on normal, osteopenia, and osteoporosis groups. BMD=bone mineral density; ICV=intracranial cavity volume; BPV=brain parenchymal volume; LVV=lateral ventricles volume.

Accordingly, we excluded patients with a history of Alzheimer's disease and other types of dementia to investigate the relationships between bone mineral density and cerebral atrophy in healthy individuals.

According to the studies mentioned previously, we hypothesized that normal aging may lead firstly to brain parenchymal atrophy and then ventricular dilatation later in normal aging-related cerebral atrophy. In addition, according to our findings, we also postulate that osteoporosis may have a role in the acceleration of parenchymal atrophy (cortical atrophy) in the early-stages of normal aging-related cerebral atrophy and ventricular enlargement (subcortical atrophy) in the late-stages. Similar to our findings, a previous study reported that BMD is reduced in the earliest clinical stages of Alzheimer's disease in both men and women [17].

Osteoporosis is a systemic disease that affects bone mass and microarchitecture throughout the body [10]. Moreover, osteoporosis is strongly associated with genetic components of type 1 collagen such as *COL1A1* and *COL1A2* [11]. Polymorphisms in COL1A1 can result in low bone density properties in individuals in early puberty, indicating that it may have potential physiological effects on bone turnover and collagen metabolism [18]. It is well documented that type 1 collagen is a major component of bone; moreover, skin, tendons, vascular smooth muscle, and other organs are also composed of type 1 collagen to varying extents. A previous study revealed that morphometric changes in the cortical capillary network occur in Alzheimer's disease in a region-specific manner, and that this phenomenon may be related to cortical atrophy in the affected regions [19]. Cerebral microvascular abnormalities have been reported as playing a role in the pathogenesis of Alzheimer's disease [20–24]. Previous studies have consistently found that a low BMD correlates with increased arterial stiffness and atherosclerosis, especially in postmenopausal women,

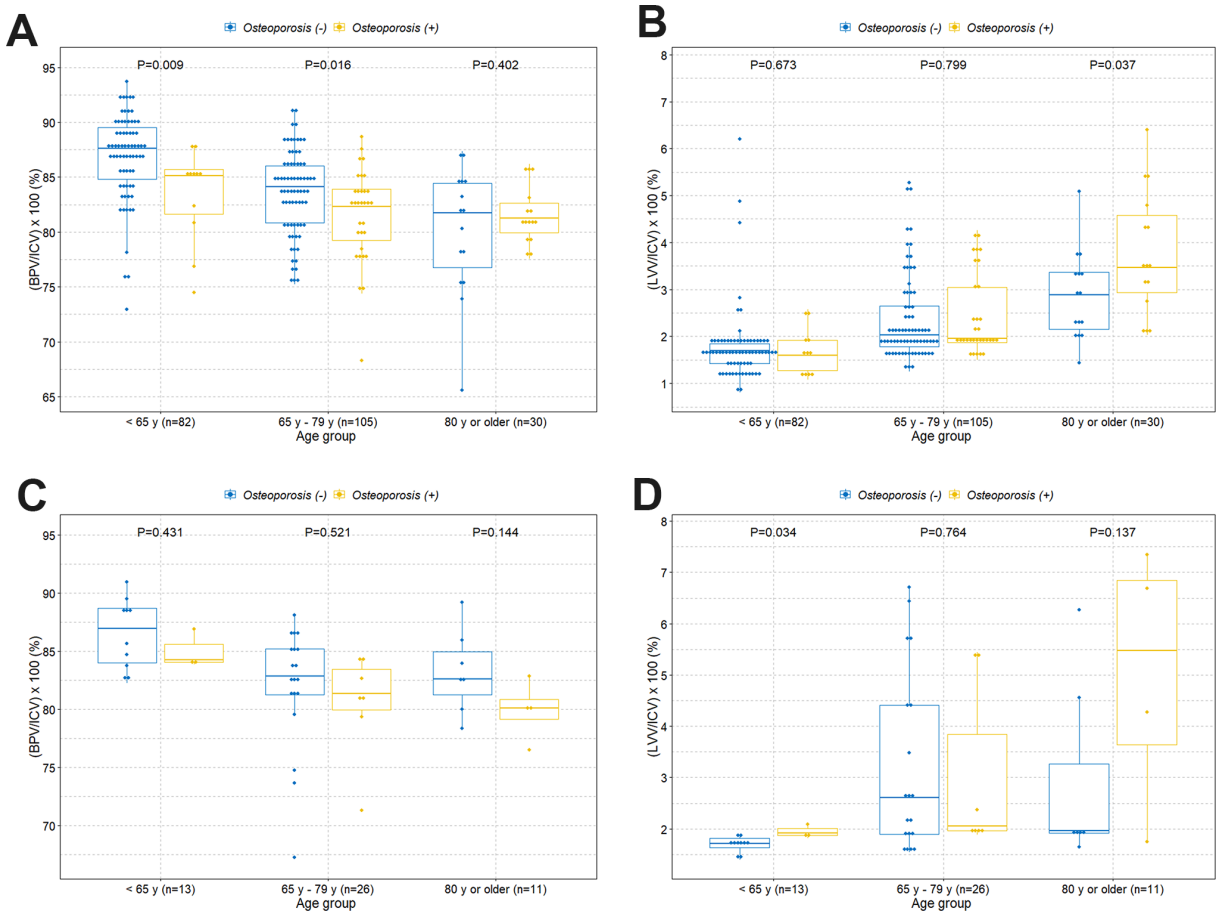

Figure 3. Boxplots with dot plots of the volume percentages of brain parenchyma and lateral ventricles classified by age groups according to osteoporosis based on sex group. (**A**) Volume percentage of brain parenchyma to intracranial cavity in females; (**B**) volume percentage of lateral ventricles to intracranial cavity in females; (**C**) volume percentage of brain parenchyma to intracranial cavity in males; (**D**) volume percentage of lateral ventricles to intracranial cavity in males. ICV=intracranial cavity volume; BPV=brain parenchymal volume; LVV=lateral ventricles volume.

who are more vulnerable to osteoporosis [25–28]. Therefore, we hypothesized that an osteoporotic condition with a strong genetic component (i.e., dysregulated type 1 collagen genes) and leads to systemic disease may also cause the degeneration of vascular smooth muscle cells, including the cortical capillary network that is also composed of type 1 collagen.

In addition, both the arachnoid trabeculae and granulations are composed of type 1 collagen, which is also the principal component of the bone matrix protein [3]. The arachnoid trabeculae is composed of abundant strands of collagen tissue that connects and brings stability to the subarachnoid space and cerebrospinal fluid flow [29]. Osteogenesis imperfecta, which is caused by mutations in the type 1 procollagen genes (COL1A1/COL1A2), is associated with communicating hydrocephalus [6, 7]. We previously hypothesized that systemic osteoporosis may negatively affect the integrity of arachnoid trabeculae and granulation, which are also composed of type 1 collagen [30]. Therefore, we hypothesized that a greater weakening of the arachnoid trabeculae and granulation in osteoporotic individuals, may accelerate the ventricular enlargement in the late-stage of normal aging-related cerebral atrophy.

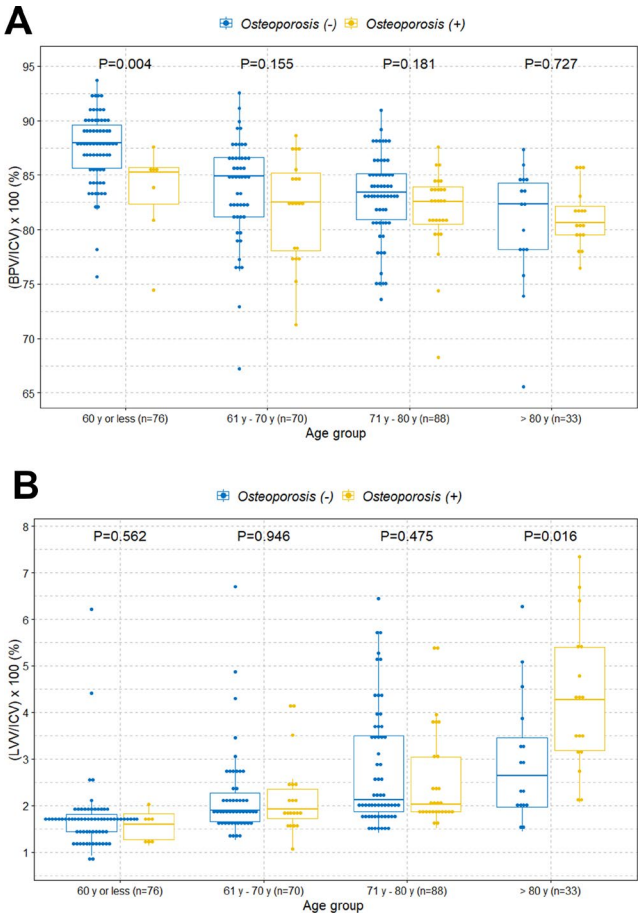

Figure 4. Boxplots with dot plots of the volume percentages of brain parenchyma and lateral ventricles classified by different age groups according to osteoporosis. (**A**) Volume percentage of brain parenchyma to intracranial cavity; (**B**) volume percentage of lateral ventricles to intracranial cavity. ICV=intracranial cavity volume; BPV=brain parenchymal volume; LVV=lateral ventricles volume.

Consistent with a previous study, we also observed that diabetes was associated with brain parenchymal atrophy [31]. In addition, our findings showed that lower BMI was associated with cerebral ventricular enlargement. As our study also showed a positive association between T-score and BMI, it is generally accepted that BMI and bone mineral density are positively correlated [32, 33]. Therefore, we believe that BMI is more linearly negatively associated with ventricle volume in all age groups, whereas BMD is negatively associated with ventricle volume, especially in the older age group.

Our study has some limitations. First, because of the study's retrospective nature, the interval between undergoing DXA and brain MRI was not consistent between all participants. A previous study found that osteoporosis develops in less than 10% of older women (≥65 years) over BMD rescreening intervals of approximately 15 years, 5 years, and 1 year for women with normal bone density, moderate osteopenia, and advanced osteopenia, respectively [34]. On the basis of this finding of the relatively slow osteoporosis progression in older women, our maximum time interval of 3 years between DXA and brain MRI may be acceptable for analysis. Second, technical errors may have occurred during measurement of brain parenchyma and lateral ventricles volumes with the 3D slicer. Third, structural changes in the brain may affect skeletal system structure and functions. Previous studies reported on the possible role of the nervous system in bone mass control [35–38]. According to these studies, brain parenchymal atrophy and ventricular enlargement may affect bone remodelling and cause osteoporosis; this fact can affect our study results. However, this mechanism is hypothetical and further studies in humans are required. In addition, we believe that our study is valuable because, to the best of our knowledge, there have been no previous clinical studies investigating the association between BMD and brain atrophy and ventricle enlargement in the elderly. We assessed the quantitative volume measurements of intracranial cavity, brain parenchyma, and lateral ventricles of participants using 3D reconstructed brain MRI images. Lastly, we included only Korean individuals, which may limit the generalizability of the results. However, data accuracy owing to consistent environmental conditions is a strength of a single-center study.

Table 6. Characteristics of the study individuals classified by age group.

Characteristics	< 65 y	65 y–79 y	80 y or older	Total	P
Number	95	131	41	267	
Sex, female, n (%)	82 (86.3)	105 (80.2)	30 (73.2)	217 (81.3)	0.177
Time interval between brain MRI and DXA, median (IQR), days	193.0 (20.0–577.0)	168.0 (40.0–473.0)	191.0 (26.5–321.5)	184.0 (33.0–441.0)	0.315
ICV, mean ± SD, cc	1240.5 ± 83.3	1221.0 ± 94.4	1201.5 ± 94.2	1224.9 ± 91.2	0.016
BPV, mean ± SD, cc	1071.0 ± 82.9	1010.0 ± 94.6	975.3 ± 97.4	1026.4 ± 97.3	< 0.001
LVV, mean ± SD, cc	22.1 ± 10.0	31.0 ± 14.7	40.3 ± 17.1	29.3 ± 15.0	< 0.001
(BPV/ICV)×100, mean ± SD, %	86.4 ± 4.0	82.7 ± 4.3	81.1 ± 4.2	83.8 ± 4.6	< 0.001
(LVV/ICV)×100, mean ± SD, %	1.8 ± 0.7	2.5 ± 1.2	3.4 ± 1.5	2.4 ± 1.2	< 0.001
(BPV/ICV)×100, median (IQR), %	87.1 (84.3–88.8)	83.2 (80.5–85.4)	81.4 (78.8–84.1)	84.2 (81.0–87.1)	< 0.001
(LVV/ICV)×100, median (IQR), %	1.7 (1.4–1.9)	2.0 (1.8–3.0)	3.2 (2.0–4.3)	1.9 (1.7–2.7)	< 0.001
T-score, mean ± SD	-1.1 ± 1.2	-1.8 ± 1.1	-2.3 ± 1.0	-1.6 ± 1.2	< 0.001
BMI, mean ± SD, kg/m^2	23.7 ± 3.5	24.8 ± 3.7	22.1 ± 2.7	24.0 ± 3.6	0.233
Hypertension, n (%)	21 (22.1)	79 (60.3)	30 (73.2)	130 (48.7)	< 0.001
Diabetes, n (%)	26 (27.4)	48 (36.6)	13 (31.7)	87 (32.6)	0.337
Alcohol, n (%)	18 (18.9)	11 (8.4)	5 (12.2)	34 (12.7)	0.063
Smoking, n (%)	11 (11.6)	9 (6.9)	3 (7.3)	23 (8.6)	0.437

SD: standard deviation; MRI: magnetic resonance imaging; DXA: dual-energy X-ray absorptiometry; IQR: interquartile range; ICV: intracranial cavity volume; BPV: brain parenchymal volume; LVV: lateral ventricles volume; BMI: body mass index.

In summary, we observed a significant linear association between BMD and brain parenchymal atrophy. We believe that osteoporosis may have a role in the acceleration of parenchymal atrophy in the early-stages of normal aging-related cerebral atrophy and ventricular enlargement in the late-stages of normal aging-related cerebral atrophy. We expect the findings of this study will expand our understanding of the association between osteoporosis and brain atrophy.

MATERIALS AND METHODS

Study design

We retrospectively recruited individuals who underwent both brain MRI and DXA at least once for any reason in our hospital from January 1, 2008 to December 31, 2018. We initially identified 3,612 individuals whose records indicated one or more procedure codes for DXA and brain MRI simultaneously. In individuals who underwent DXA more than once, the lowest T-score from among the multiple DXA T-score values was considered. If multiple MRIs were performed, we considered that which was performed closest to the date of the DXA with the lowest T-score. We then excluded 3,345 individuals using stepwise methods for the following reasons: (1) more than 3 years elapsed between DXA and brain MRI (to reduce time heterogeneity) (n=683); (2) individuals in whom a brain MRI did not include T1-weighted axial multiplanar reconstruction (MPR) sequence (3-mm-thick slices) (n=2192); and (3) history of Alzheimer's disease, other types of dementia, brain surgery, brain tumor (intra-axial, extra-axial, metastasis, leptomeningeal metastasis), stroke (ischemic, hemorrhagic), traumatic brain injury, brain infections (meningitis, abscess, neurocysticercosis), multiple sclerosis, and arachnoid cyst (n=470). Ultimately, we enrolled 267 individuals with no history of Alzheimer's disease, other types of dementia, brain surgery, brain tumor, stroke, traumatic brain injury, brain infections, multiple sclerosis, or arachnoid cysts who underwent one or more DXA and brain MRI (included 3D T1-weighted multiplanar reconstruction (MPR) sequence), within 3 years of each other at our hospital over an 11-year period (Figure 5).

This study was approved by the Institutional Review Board of Hanyang University Guri Hospital, Korea, and conformed to the tenets of the Declaration of Helsinki. Owing to the retrospective nature of the study, the need for informed consent was waived. All individual records were anonymized prior to analysis.

BMD measurement

DXA to assess the BMC (g) and BMD (g/cm^2) of the lumbar spine L1–L4 and femoral neck was performed using a Discovery Wi DXA system (Hologic, Bedford, MA) in all study subjects. All testing was conducted by licensed technicians. The BMD values were converted into a T- and Z-score. T-score reference ranges were calculated using data from healthy young Asian women provided by the bone densitometry equipment manufacturer. Z-Scores were also calculated from the mean BMD of a healthy Asian population of the same age and sex. Study individuals were categorized as normal, osteopenia, or osteoporosis based on the World Health Organization T-score classification: osteoporosis was defined as a T-score (≤ -2.5), osteopenia as a T-score > -2.5 and ≤ -1.0), and normal BMD as a T-score > -1.0. The lower T-score value between the lumbar spine and femoral neck was adopted as the T-score for the study.

Brain MRI image acquisition

All 3D T1-weighted MPR MR images (slice thicknesses, 1.5-3.0 mm) were obtained with an Ingenia 3.0 Tesla CX (Philips Ingenia, Philips Medical Systems, Böblingen, Germany) and Achieva 3.0 Tesla TX (Philips Achieva, Philips Medical Systems, Böblingen, Germany) scanners at our hospital. Technical parameters were standardized as following; TE: 4.61 ms; TR: 8.29 ms; field of view: 207 × 207 mm; matrix size: 224*224 pixels. A previous study described that MPR sequences with a 3.0 Tesla MRI provided excellent visualization for the inner structures of head and brain [39].

Volumetric assessment of intracranial cavity, brain parenchyma, and lateral ventricles

We measured ICV, BPV, and LVV with a 3D slicer software in its latest version, 4.10.1. (http://www.slicer.org). The reliability of the 3D slicer has been described elsewhere, including detailed descriptions of the slicer's various functions [40, 41].

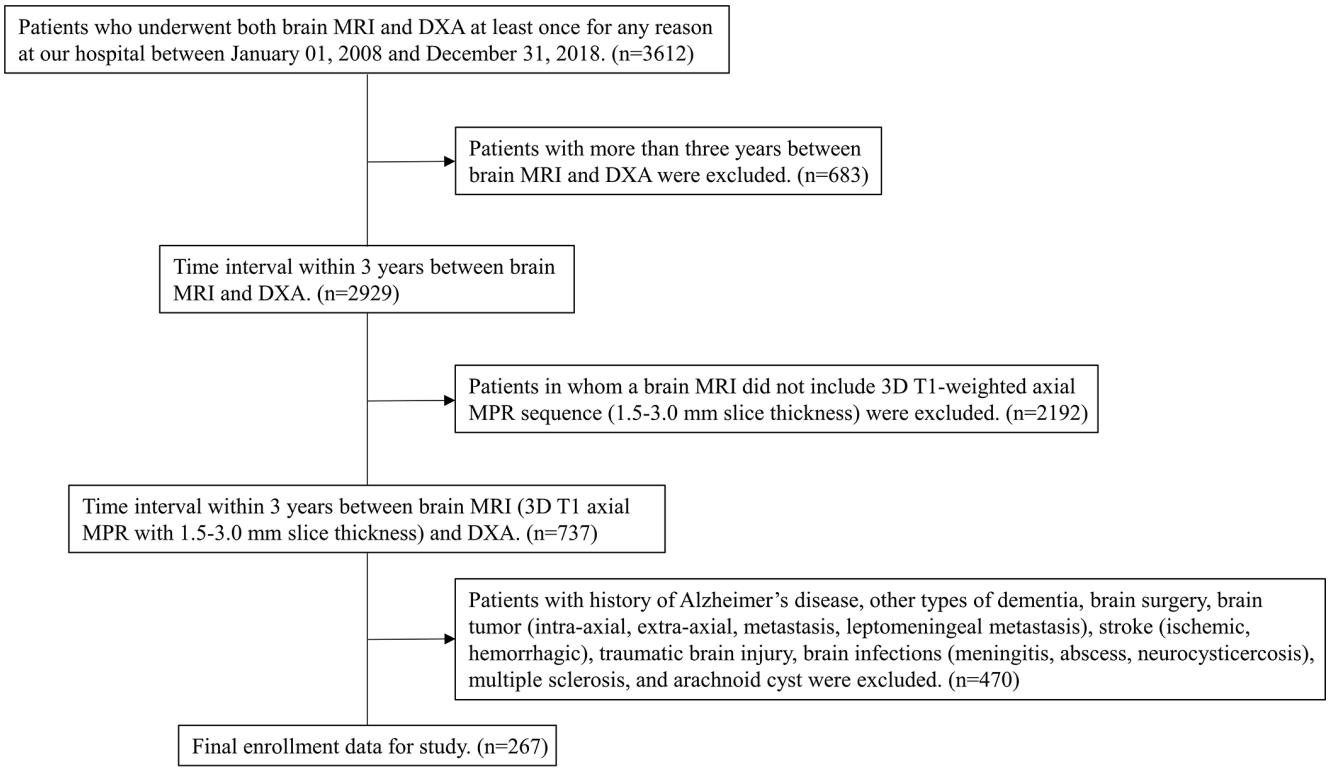

Figure 5. Flow chart of the process for selecting eligible patients from individuals who underwent both brain MRI and DXA in our hospital during the period of January 1, 2008, to December 31, 2018. MRI=magnetic resonance imaging; DXA=dual-energy X-ray absorptiometry; MPR=multiplanar reconstruction.

All procedures were performed by a well-trained 3D-slicer user. The T1-weighted MR images were used for the analysis in all study individuals as T1-weighted MR imaging is appropriate for skull stripping (https://www.slicer.org/wiki/Modules:SkullStripperModule) and the measurement of brain parenchyma and CSF space volumes using a slicer [42]. In addition, as the T1 MPR sequence with the 3.0 Tesla MRI in our hospital showed a relatively thin slice thickness of 1.5–3.0 mm, we were able to perform more accurate volumetric measurements.

The stepwise methods of volumetric assessment using 3D slicer were as follows: (1) brain MRI DICOM files from the picture archiving and communication system (PACS) were loaded to the software; (2) Swiss Skull Stripper function was used to strip off the skull from the loaded MRI to segment intracranial cavity; (3) threshold-based methods were then used to segment the brain parenchyma and lateral ventricles; (4) 3D reconstruction was performed using the Model Maker function; and (5) Label Statistics function was used to calculate the ICV, BPV, and LVV (Figure 6). Further detailed techniques are presented in Supplementary Figures 5–7.

Medical variables

All medical information of the enrolled subjects was investigated by a trained research member using all medical charts, including nurse records. Age was defined as the age at the time of MRI. The individuals' weight and height were investigated at or near the time of MRI from the medical records. BMI was calculated as weight/(height × height) and expressed in kg/m^2. Medical history of hypertension, diabetes, alcohol drinking, and smoking at or near the time of MRI was also evaluated. A history of smoking and drinking was defined to include current smokers and drinkers (but not former smokers and drinkers).

Statistical methods

Continuous variables are expressed as mean ± SD or median with interquartile range, while discrete variables are expressed as a count and percentage. The chi-square test and Student's *t*-test were used to assess clinical differences between two groups. Statistical comparison between age groups was performed using one-way ANOVA followed by Tukey's test (Tables 2 and 6).

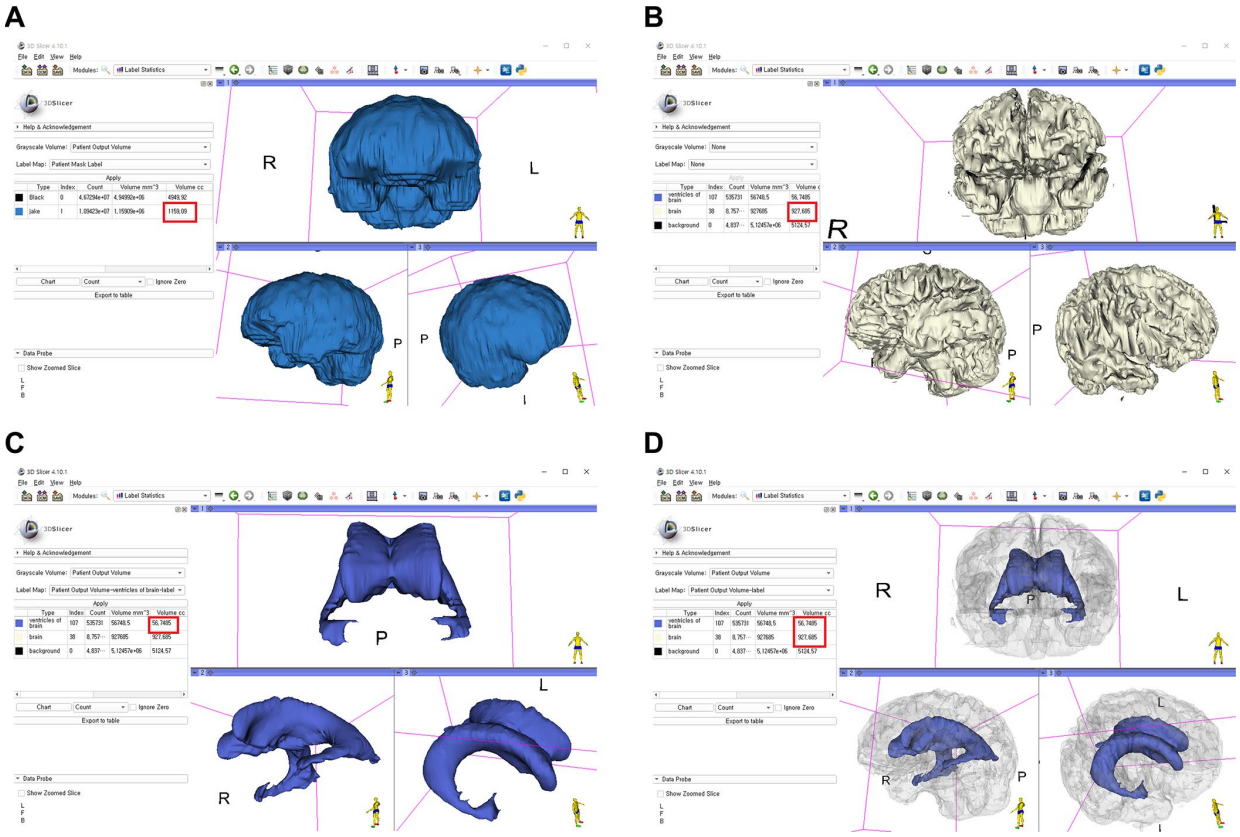

Figure 6. Segmentation of the intracranial cavity, brain parenchyma, and lateral ventricles with a 3D-reconstructed model using the 3D slicer and calculation of each volume (red box indicates the volume). (**A**) Intracranial cavity; (**B**) brain parenchyma; (**C**) lateral ventricles; (**D**) merge of the brain parenchyma and lateral ventricles.

Pearson correlation coefficients with/without adjustment for age were calculated to evaluate the relationships between volume percentage of brain parenchyma and lateral ventricles and bone densitometric parameters.

The intracranial cavity volume percentages of brain parenchyma and lateral ventricles were calculated as (BPV/ICV) × 100% and (LVV/ICV) × 100%, respectively. We constructed scatterplots with a regression line to represent the association between T-scores and the intracranial cavity volume percentages of brain parenchyma and lateral ventricles. Multivariable linear regression was also performed to identify independent associations between T-scores and the intracranial cavity volume percentages of the brain parenchyma and lateral ventricles. In addition to the T-score, covariates, including sex, age at the time of brain MRI (continuous variable), time interval between brain MRI and DXA (continuous variable), BMI (continuous variable), hypertension, diabetes, alcohol, and smoking were entered into the multi-variable model.

Box plots with dot plots were used to visualize the association between the intracranial cavity volume percentages of brain parenchyma and lateral ventricles, and age groups according to with or without osteoporosis. P-values less than 0.05 were considered statistically significant.

All statistical analyses were performed using R version 3.5.2 (https://www.r-project.org/).

Abbreviations

BMD: bone mineral density; DXA: dual-energy X-ray absorptiometry; ICV: intracranial cavity volume; BPV: brain parenchymal volume; LVV: lateral ventricles volume; MRI: magnetic resonance imaging; MPR: multiplanar reconstruction.

AUTHOR CONTRIBUTIONS

I.S.B. and M.H.H. conceived and designed this research. I.S.B collected data and performed imaging analysis. M.H.H. performed statistical analyses and data interpretation and analysis for this article. J.I.R., J.H.C., and J.M.K. were involved in critical review for this article. I.S.B. and M.H.H. wrote the manuscript. J.I.R., J.H.C., and J.M.K. provided administrative, technical, or material support. All authors edited and approved the final manuscript.

CONFLICTS OF INTEREST

There are no conflicts of interest to be declared.

FUNDING

This work was supported by the research fund of Hanyang University (HY- 201800000002600)

REFERENCES

1. Apostolova LG, Green AE, Babakchanian S, Hwang KS, Chou YY, Toga AW, Thompson PM. Hippocampal atrophy and ventricular enlargement in normal aging, mild cognitive impairment (MCI), and Alzheimer Disease. Alzheimer Dis Assoc Disord. 2012; 26:17–27. https://doi.org/10.1097/WAD.0b013e3182163b62 PMID:22343374

2. Scahill RI, Frost C, Jenkins R, Whitwell JL, Rossor MN, Fox NC. A longitudinal study of brain volume changes in normal aging using serial registered magnetic resonance imaging. Arch Neurol. 2003; 60:989–94. https://doi.org/10.1001/archneur.60.7.989 PMID:12873856

3. Saboori P, Sadegh A. Histology and Morphology of the Brain Subarachnoid Trabeculae. Anat Res Int. 2015; 2015:279814. https://doi.org/10.1155/2015/279814 PMID:26090230

4. Young MF. Bone matrix proteins: their function, regulation, and relationship to osteoporosis. Osteoporos Int. 2003 (Suppl 3); 14:S35–42. https://doi.org/10.1007/s00198-002-1342-7 PMID:12730768

5. Díaz JA, Murillo MF, Jaramillo NA. Framework of collagen type I - vasoactive vessels structuring invariant geometric attractor in cancer tissues: insight into biological magnetic field. PLoS One. 2009; 4:e4506. https://doi.org/10.1371/journal.pone.0004506 PMID:19223987

6. Rolvien T, Kornak U, Stürznickel J, Schinke T, Amling M, Mundlos S, Oheim R. A novel COL1A2 C-propeptide cleavage site mutation causing high bone mass osteogenesis imperfecta with a regional distribution pattern. Osteoporos Int. 2018; 29:243–46. https://doi.org/10.1007/s00198-017-4224-8 PMID:28916840

7. Charnas LR, Marini JC. Communicating hydrocephalus, basilar invagination, and other neurologic features in osteogenesis imperfecta. Neurology. 1993; 43:2603–08. https://doi.org/10.1212/WNL.43.12.2603 PMID:8255464

8. Albayram S, Kizilkilic O, Yilmaz H, Tuysuz B, Kocer N, Islak C. Abnormalities in the cerebral arterial system in osteogenesis imperfecta. AJNR Am J Neuroradiol. 2003; 24:748–50. PMID:12695216

9. Folkestad L, Hald JD, Gram J, Langdahl BL, Hermann AP, Diederichsen AC, Abrahamsen B, Brixen K. Cardiovascular disease in patients with osteogenesis imperfecta - a nationwide, register-based cohort study. Int J Cardiol. 2016; 225:250–57. https://doi.org/10.1016/j.ijcard.2016.09.107 PMID:27741483

10. Brandi ML. Microarchitecture, the key to bone quality. Rheumatology (Oxford). 2009 (Suppl 4); 48:iv3–8. https://doi.org/10.1093/rheumatology/kep273 PMID:19783591

11. Grant SF, Reid DM, Blake G, Herd R, Fogelman I, Ralston SH. Reduced bone density and osteoporosis associated with a polymorphic Sp1 binding site in the collagen type I alpha 1 gene. Nat Genet. 1996; 14:203–05. https://doi.org/10.1038/ng1096-203 PMID:8841196

12. Kaye JA, DeCarli C, Luxenberg JS, Rapoport SI. The significance of age-related enlargement of the cerebral ventricles in healthy men and women measured by quantitative computed X-ray tomography. J Am Geriatr Soc. 1992; 40:225–31. https://doi.org/10.1111/j.1532-5415.1992.tb02073.x PMID:1538040

13. Fox NC, Schott JM. Imaging cerebral atrophy: normal ageing to Alzheimer's disease. Lancet. 2004; 363: 392–94. https://doi.org/10.1016/S0140-6736(04)15441-X PMID:15074306

14. Yamada S, Asano T, Enomoto M, Sakata M, Tanno M, Yamada H, Esaki Y, Mizutani T. Ventricular dilatation and brain atrophy of normal elderly individuals and patients with Alzheimer-type dementia: A retrospective longitudinal computed tomographic study of autopsy cases. Neuropathology. 1998; 18:261–69. https://doi.org/10.1111/j.1440-1789.1998.tb00113.x

15. Nestor SM, Rupsingh R, Borrie M, Smith M, Accomazzi V, Wells JL, Fogarty J, Bartha R, and Alzheimer's Disease Neuroimaging Initiative. Ventricular enlargement as a possible measure of Alzheimer's disease progression validated using the Alzheimer's disease neuroimaging initiative database. Brain. 2008; 131:2443–54. https://doi.org/10.1093/brain/awn146 PMID:18669512

16. Toepper M. Dissociating Normal Aging from Alzheimer's Disease: A View from Cognitive Neuroscience. J Alzheimers Dis. 2017; 57:331–52. https://doi.org/10.3233/JAD-161099 PMID:28269778

17. Loskutova N, Honea RA, Vidoni ED, Brooks WM, Burns JM. Bone density and brain atrophy in early Alzheimer's disease. J Alzheimers Dis. 2009; 18:777–85. https://doi.org/10.3233/JAD-2009-1185 PMID:19661621

18. Suuriniemi M, Kovanen V, Mahonen A, Alén M, Wang Q, Lyytikäinen A, Cheng S. COL1A1 Sp1 polymorphism associates with bone density in early puberty. Bone. 2006; 39:591–97. https://doi.org/10.1016/j.bone.2006.02.053 PMID:16580273

19. Richard E, van Gool WA, Hoozemans JJ, van Haastert ES, Eikelenboom P, Rozemuller AJ, van de Berg WD. Morphometric Changes in the Cortical Microvascular Network in Alzheimer's Disease. J Alzheimers Dis. 2010; 22:811–18. https://doi.org/10.3233/JAD-2010-100849 PMID:20858968

20. Dickstein DL, Walsh J, Brautigam H, Stockton SD Jr, Gandy S, Hof PR. Role of vascular risk factors and vascular dysfunction in Alzheimer's disease. Mt Sinai J Med. 2010; 77:82–102. https://doi.org/10.1002/msj.20155 PMID:20101718

21. Buée L, Hof PR, Bouras C, Delacourte A, Perl DP, Morrison JH, Fillit HM. Pathological alterations of the cerebral microvasculature in Alzheimer's disease and related dementing disorders. Acta Neuropathol. 1994; 87:469–80. https://doi.org/10.1007/BF00294173 PMID:8059599

22. Zlokovic BV. Neurovascular mechanisms of Alzheimer's neurodegeneration. Trends Neurosci. 2005; 28:202–08. https://doi.org/10.1016/j.tins.2005.02.001 PMID:15808355

23. Challa VR, Thore CR, Moody DM, Anstrom JA, Brown WR. Increase of white matter string vessels in Alzheimer's disease. J Alzheimers Dis. 2004; 6:379–83. https://doi.org/10.3233/jad-2004-6404 PMID:15345807

24. Farkas E, Luiten PG. Cerebral microvascular pathology in aging and Alzheimer's disease. Prog Neurobiol. 2001; 64:575–611. https://doi.org/10.1016/S0301-0082(00)00068-X PMID:11311463

25. El-Bikai R, Tahir MR, Tremblay J, Joffres M, Šeda O, Šedová L, Awadalla P, Laberge C, Knoppers BM, Dumas P, Gaudet D, Ste-Marie LG, Hamet P. Association of age-dependent height and bone mineral density decline with increased arterial stiffness and rate of fractures in hypertensive individuals. J Hypertens. 2015; 33:727–35.

https://doi.org/10.1097/HJH.0000000000000475 PMID:25915877

26. Sumino H, Ichikawa S, Kasama S, Takahashi T, Kumakura H, Takayama Y, Kanda T, Sakamaki T, Kurabayashi M. Elevated arterial stiffness in postmenopausal women with osteoporosis. Maturitas. 2006; 55:212–18. https://doi.org/10.1016/j.maturitas.2006.02.008 PMID:16621356

27. Kanis JA, McCloskey EV, Johansson H, Cooper C, Rizzoli R, Reginster JY, and Scientific Advisory Board of the European Society for Clinical and Economic Aspects of Osteoporosis and Osteoarthritis (ESCEO) and the Committee of Scientific Advisors of the International Osteoporosis Foundation (IOF). European guidance for the diagnosis and management of osteoporosis in postmenopausal women. Osteoporos Int. 2013; 24:23–57. https://doi.org/10.1007/s00198-012-2074-y PMID:23079689

28. Shargorodsky M, Boaz M, Luckish A, Matas Z, Gavish D, Mashavi M. Osteoprotegerin as an independent marker of subclinical atherosclerosis in osteoporotic postmenopausal women. Atherosclerosis. 2009; 204:608–11. https://doi.org/10.1016/j.atherosclerosis.2008.10.024 PMID:19062016

29. Mortazavi MM, Quadri SA, Khan MA, Gustin A, Suriya SS, Hassanzadeh T, Fahimdanesh KM, Adl FH, Fard SA, Taqi MA, Armstrong I, Martin BA, Tubbs RS. Subarachnoid Trabeculae: A Comprehensive Review of Their Embryology, Histology, Morphology, and Surgical Significance. World Neurosurg. 2018; 111:279–90. https://doi.org/10.1016/j.wneu.2017.12.041 PMID:29269062

30. Han MH, Won YD, Na MK, Kim CH, Kim JM, Ryu JI, Yi HJ, Cheong JH. Association Between Possible Osteoporosis and Shunt-Dependent Hydrocephalus After Subarachnoid Hemorrhage. Stroke. 2018; 49:1850–58. https://doi.org/10.1161/STROKEAHA.118.021063 PMID:29946014

31. Roberts RO, Knopman DS, Przybelski SA, Mielke MM, Kantarci K, Preboske GM, Senjem ML, Pankratz VS, Geda YE, Boeve BF, Ivnik RJ, Rocca WA, Petersen RC, Jack CR Jr. Association of type 2 diabetes with brain atrophy and cognitive impairment. Neurology. 2014; 82:1132–41. https://doi.org/10.1212/WNL.0000000000000269 PMID:24647028

32. Ravn P, Cizza G, Bjarnason NH, Thompson D, Daley M, Wasnich RD, McClung M, Hosking D, Yates AJ, Christiansen C. Low body mass index is an important risk factor for low bone mass and increased bone loss in early postmenopausal women. Early Postmenopausal Intervention Cohort (EPIC) study group. J Bone Miner Res. 1999; 14:1622–27. https://doi.org/10.1359/jbmr.1999.14.9.1622 PMID:10469292

33. Kim SJ, Yang WG, Cho E, Park EC. Relationship between Weight, Body Mass Index and Bone Mineral Density of Lumbar Spine in Women. J Bone Metab. 2012; 19:95–102. https://doi.org/10.11005/jbm.2012.19.2.95 PMID:24524039

34. Gourlay ML, Fine JP, Preisser JS, May RC, Li C, Lui LY, Ransohoff DF, Cauley JA, Ensrud KE, and Study of Osteoporotic Fractures Research Group. Bone-density testing interval and transition to osteoporosis in older women. N Engl J Med. 2012; 366:225–33. https://doi.org/10.1056/NEJMoa1107142 PMID:22256806

35. Jones KB, Mollano AV, Morcuende JA, Cooper RR, Saltzman CL. Bone and brain: a review of neural, hormonal, and musculoskeletal connections. Iowa Orthop J. 2004; 24:123–32. PMID:15296219

36. Takeda S, Elefteriou F, Levasseur R, Liu X, Zhao L, Parker KL, Armstrong D, Ducy P, Karsenty G. Leptin regulates bone formation via the sympathetic nervous system. Cell. 2002; 111:305–17. https://doi.org/10.1016/S0092-8674(02)01049-8 PMID:12419242

37. Elefteriou F, Ahn JD, Takeda S, Starbuck M, Yang X, Liu X, Kondo H, Richards WG, Bannon TW, Noda M, Clement K, Vaisse C, Karsenty G. Leptin regulation of bone resorption by the sympathetic nervous system and CART. Nature. 2005; 434:514–20. https://doi.org/10.1038/nature03398 PMID:15724149

38. Elefteriou F. Regulation of bone remodeling by the central and peripheral nervous system. Arch Biochem Biophys. 2008; 473:231–36. https://doi.org/10.1016/j.abb.2008.03.016 PMID:18410742

39. Oto C, Ekim O. 3 Tesla Magnetic resonance imaging and multiplanar reconstruction of the brain and its associated structures in pig. Ank Üniversitesi Vet Fakültesi Derg. 58:73–8. https://doi.org/10.1501/vetfak_0000002453

40. Gonzalo Domínguez M, Hernández C, Ruisoto P, Juanes JA, Prats A, Hernández T. Morphological and Volumetric Assessment of Cerebral Ventricular System with 3D Slicer Software. J Med Syst. 2016; 40:154. https://doi.org/10.1007/s10916-016-0510-9 PMID:27147517

41. Ma Z, Chen X, Huang Y, He L, Liang C, Liang C, Liu Z. MR diffusion-weighted imaging-based subcutaneous tumour volumetry in a xenografted nude mouse model using 3D Slicer: an accurate and repeatable method. Sci Rep. 2015; 5:15653. Accessed March 27, 2019. https://doi.org/10.1038/srep15653 PMID:26489359

42. Alperin N, Ranganathan S, Bagci AM, Adams DJ, Ertl-Wagner B, Saraf-Lavi E, Sklar EM, Lam BL. MRI evidence of impaired CSF homeostasis in obesity-associated idiopathic intracranial hypertension. AJNR Am J Neuroradiol. 2013; 34:29–34. https://doi.org/10.3174/ajnr.A3171 PMID:22766676

SUPPLEMENTARY MATERIALS

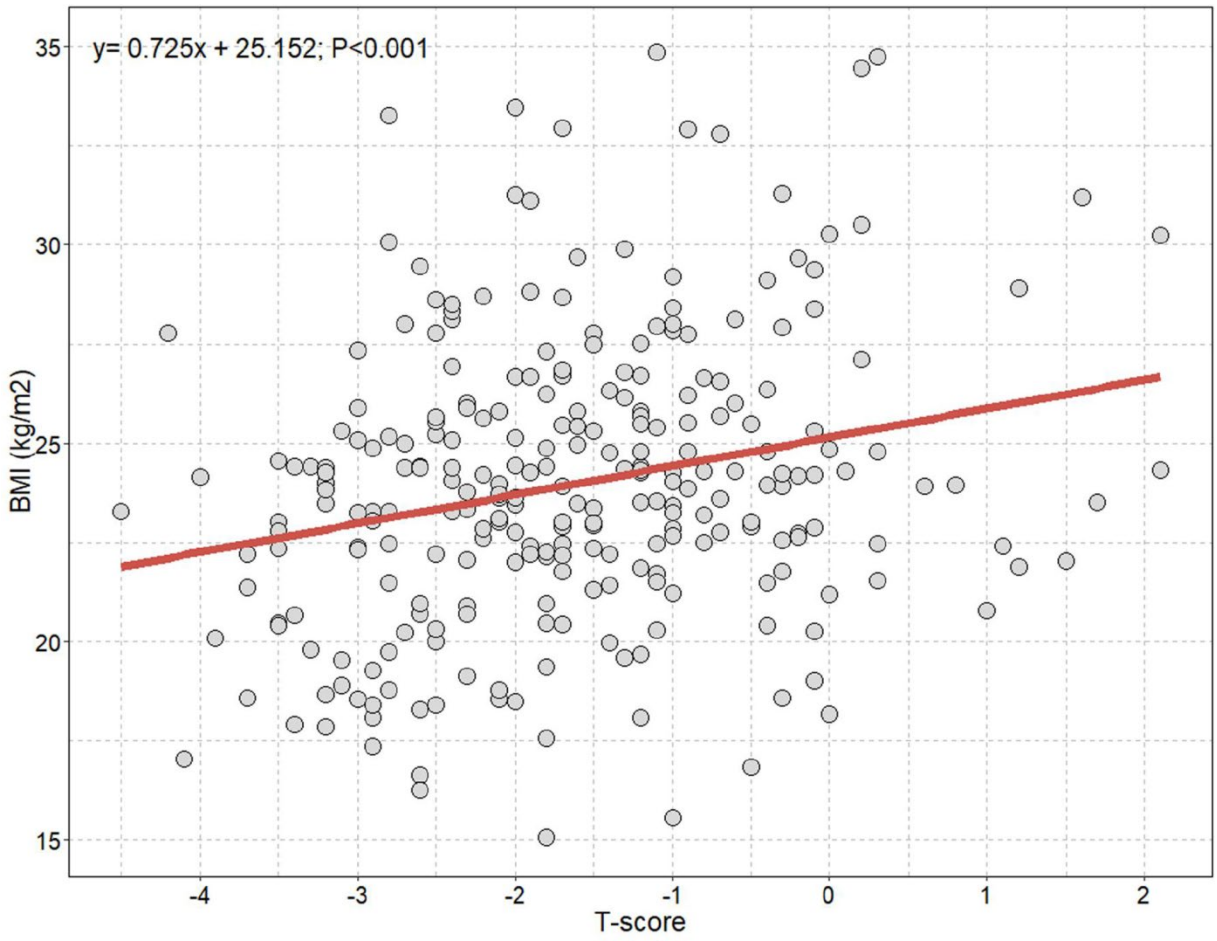

Supplementary Figure 1. Scatter plot with the linear regression line showing the association between T-score and BMI in the study individuals.

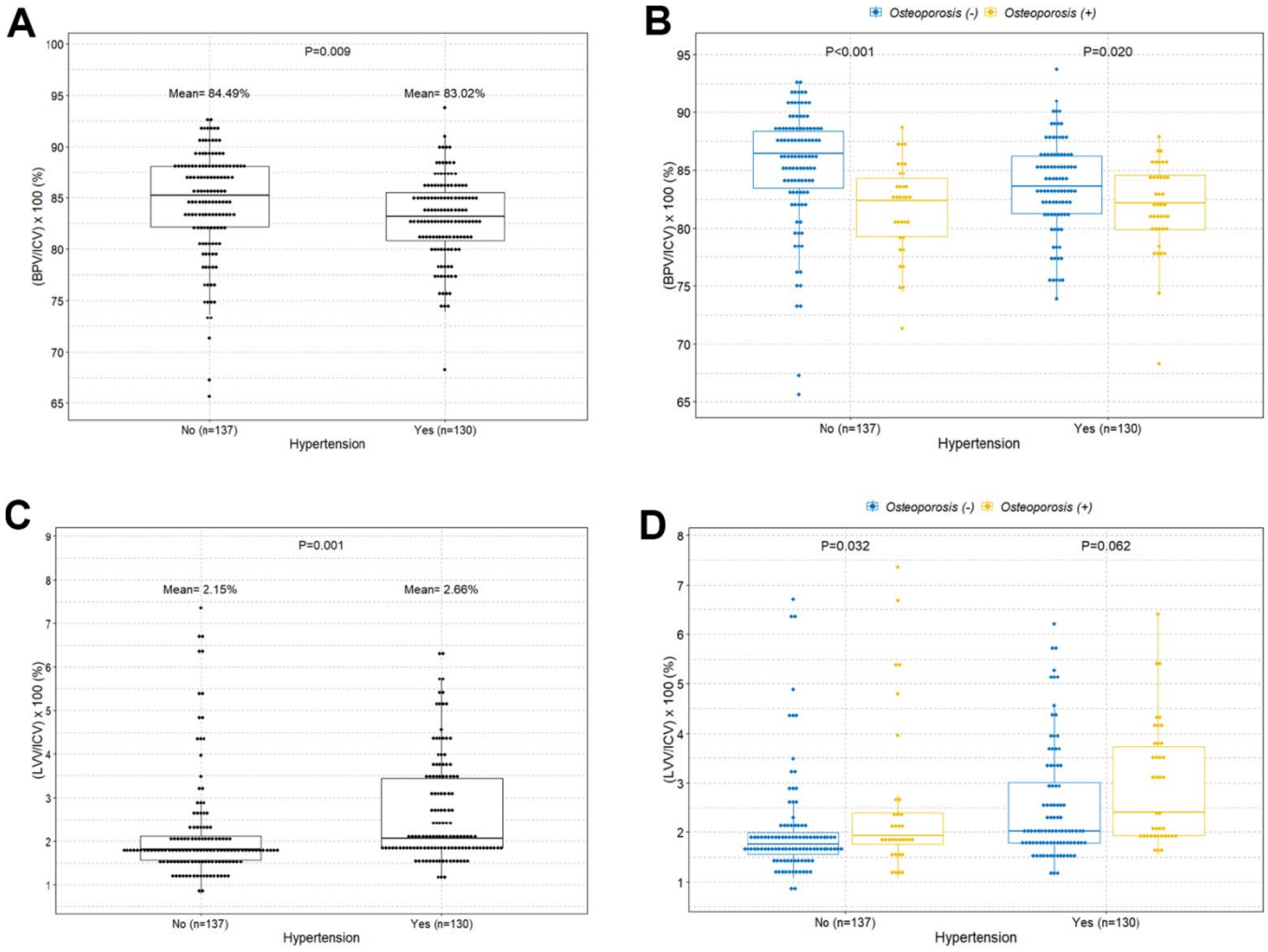

Supplementary Figure 2. Boxplots with dot plots of the volume percentages of brain parenchyma and lateral ventricles classified by history of hypertension. (**A**) volume percentage of brain parenchyma to intracranial cavity; (**B**) volume percentage of brain parenchyma to intracranial cavity according to osteoporosis; (**C**) volume percentage of lateral ventricles to intracranial cavity; (**D**) volume percentage of lateral ventricles to intracranial cavity according to osteoporosis. ICV=intracranial cavity volume; BPV=brain parenchymal volume; LVV=lateral ventricles volume.

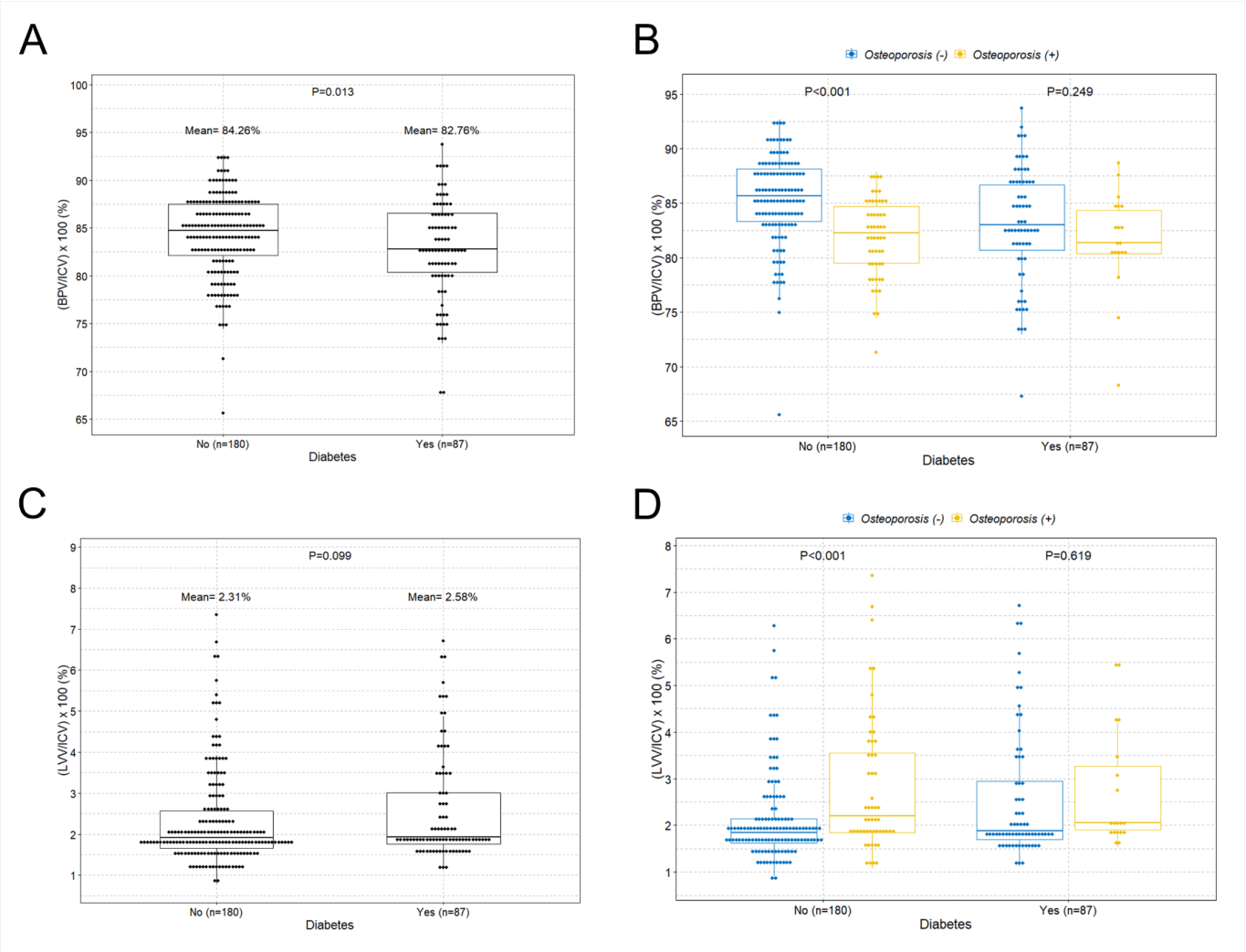

Supplementary Figure 3. Boxplots with dot plots of the volume percentages of brain parenchyma and lateral ventricles classified by history of diabetes. (**A**) volume percentage of brain parenchyma to intracranial cavity; (**B**) volume percentage of brain parenchyma to intracranial cavity according to osteoporosis; (**C**) volume percentage of lateral ventricles to intracranial cavity; (**D**) volume percentage of lateral ventricles to intracranial cavity according to osteoporosis. ICV=intracranial cavity volume; BPV=brain parenchymal volume; LVV=lateral ventricles volume.

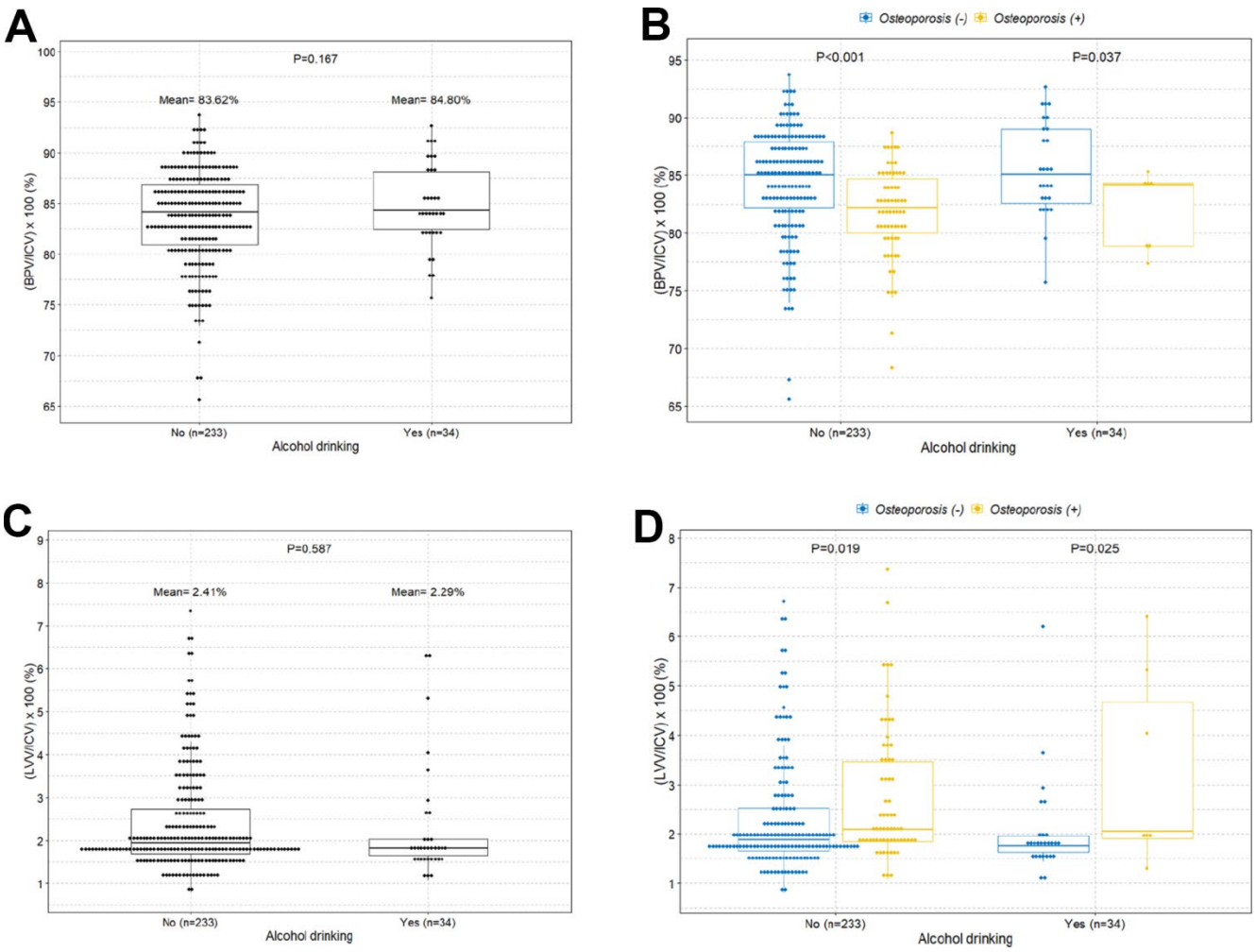

Supplementary Figure 4. Boxplots with dot plots of the volume percentages of brain parenchyma and lateral ventricles classified by history of alcohol. (**A**) volume percentage of brain parenchyma to intracranial cavity; (**B**) volume percentage of brain parenchyma to intracranial cavity according to osteoporosis; (**C**) volume percentage of lateral ventricles to intracranial cavity; (**D**) volume percentage of lateral ventricles to intracranial cavity according to osteoporosis. ICV=intracranial cavity volume; BPV=brain parenchymal volume; LVV=lateral ventricles volume.

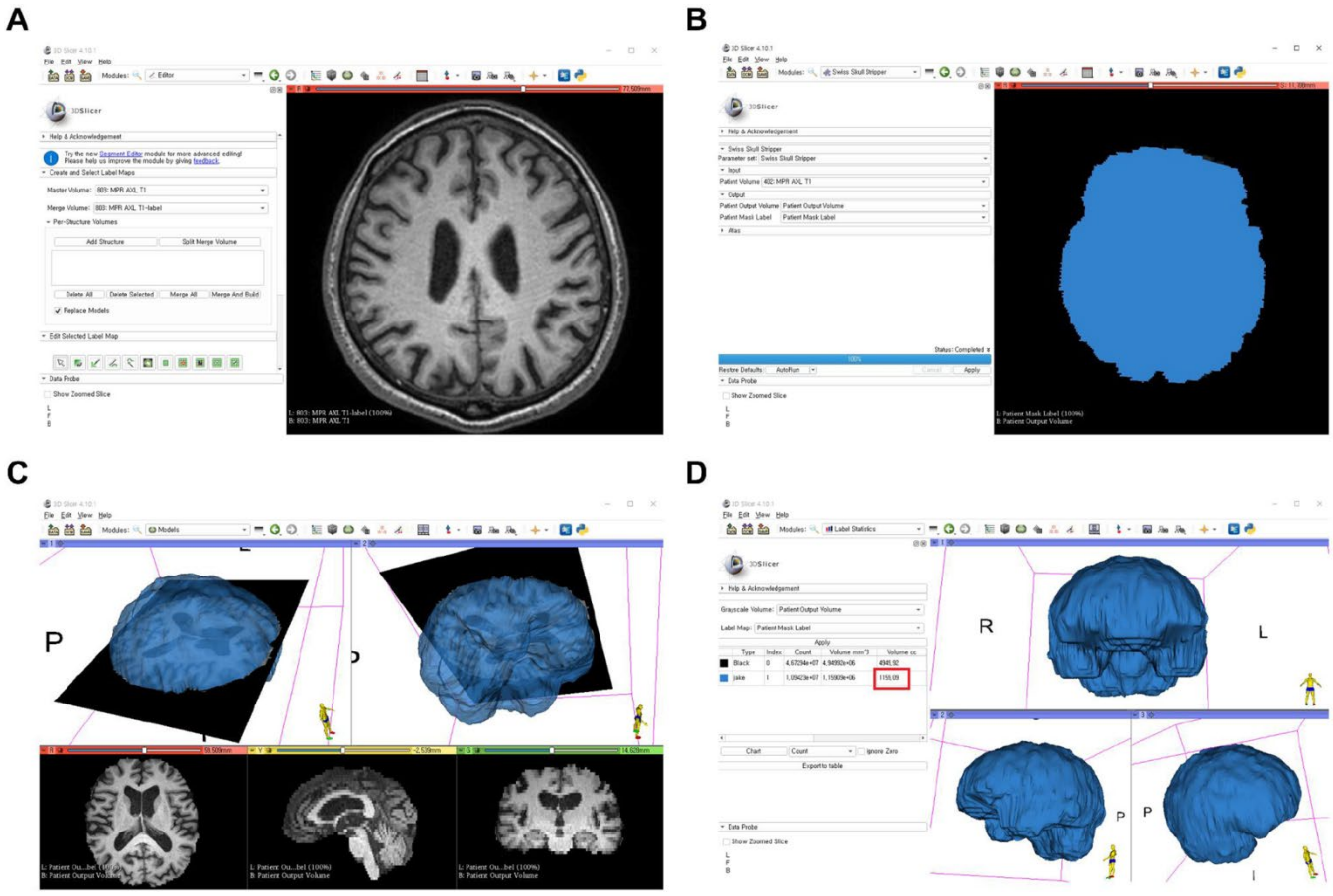

Supplementary Figure 5. Example of stepwise intracranial cavity volumetric assessment using 3D slicer. (**A**) brain MRI DICOM files from picture archiving and communication system (PACS) loading to the software; (**B**) Swiss Skull Stripper method used to segment the intracranial cavity; (**C**) 3D reconstruction was performed using the Model Maker function of the 3D slicer (**D**) Label Statistics function calculated the 3D reconstructed intracranial cavity volume.

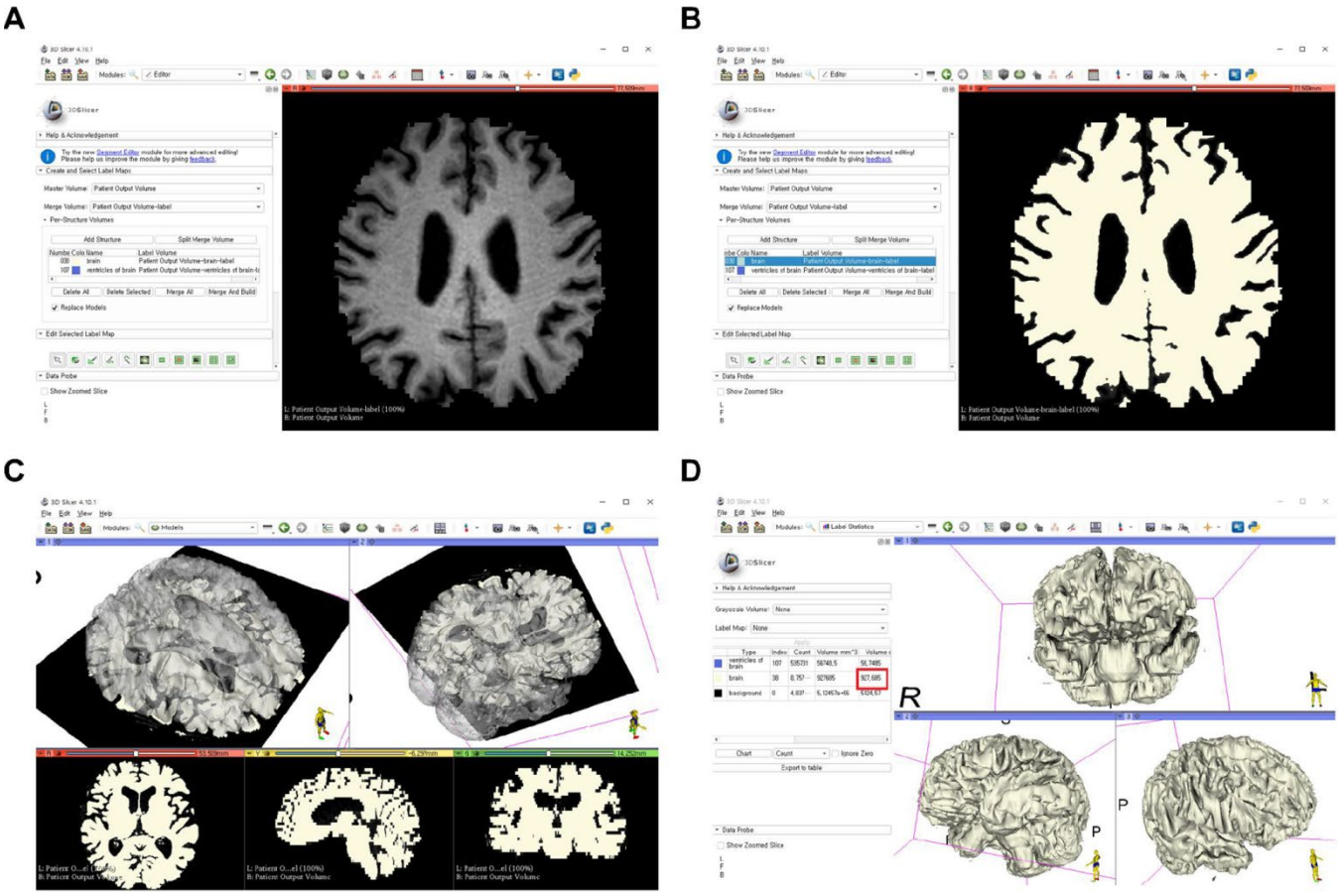

Supplementary Figure 6. Example of stepwise brain parenchyma volumetric assessment using 3D slicer. (**A**) brain MRI DICOM files from picture archiving and communication system (PACS) loading to the software. Swiss Skull Stripper method was then used to segment the intracranial cavity; (**B**) threshold-based method used to segment the brain parenchyma; (**C**) 3D reconstruction was performed using the Model Maker function of the 3D slicer (**D**) Label Statistics function calculated the 3D reconstructed brain parenchymal volume.

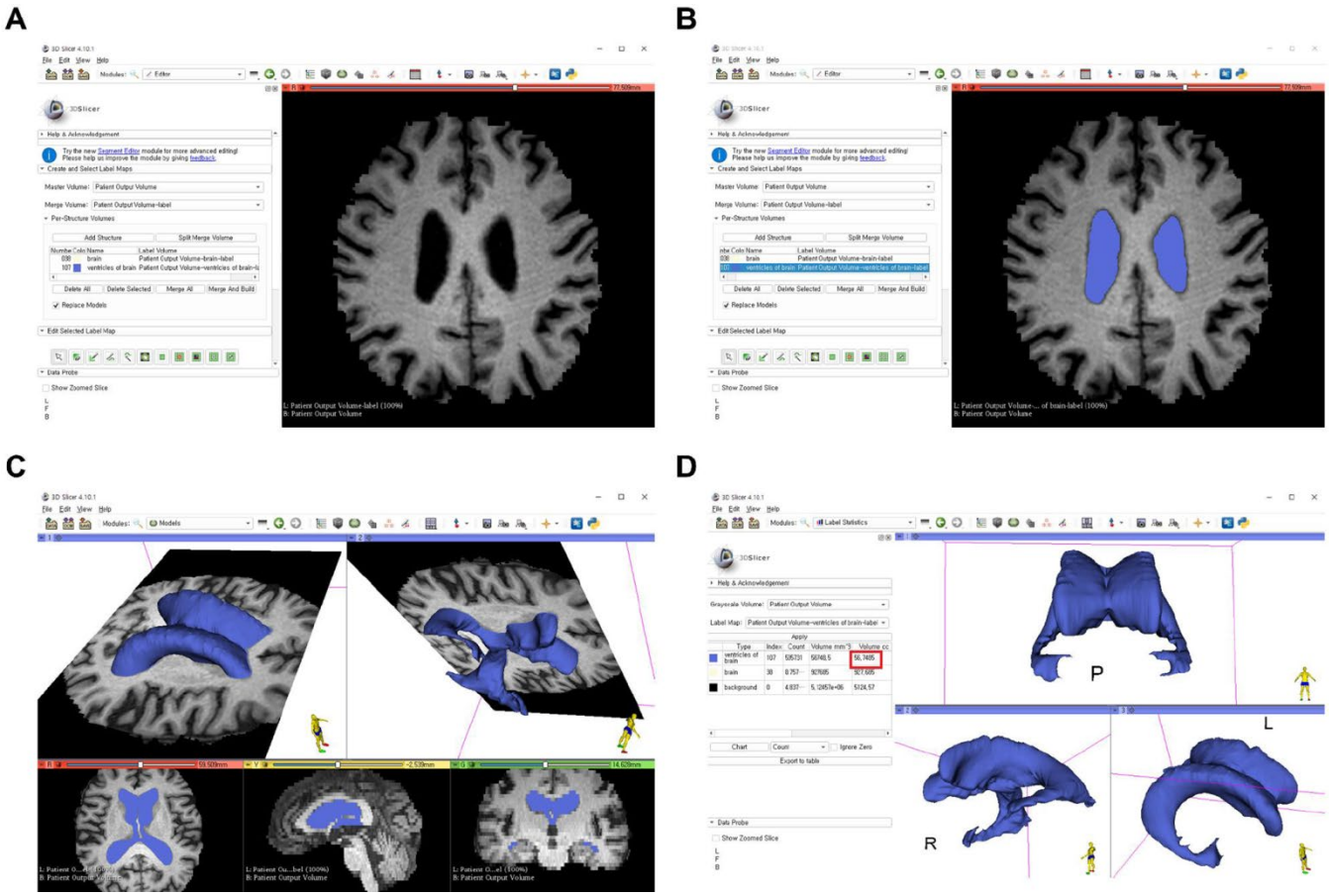

Supplementary Figure 7. Example of stepwise lateral ventricles volumetric assessment using 3D slicer. (**A**) brain MRI DICOM files from picture archiving and communication system (PACS) loading to the software. Swiss Skull Stripper method was then used to segment the intracranial cavity; (**B**) threshold-based method and Save Island function used to segment the lateral ventricles; (**C**) 3D reconstruction was performed using the Model Maker function of the 3D slicer (**D**) Label Statistics function calculated the 3D reconstructed lateral ventricles volume.